Memoirs of the Faculty of Engineering, Nagoya University
Vol. 35, No. 1 (1983) —Research Report —

COMPUTATION OF WAVE DRIFT FORCES ON FLOATING AXISYMMETRIC BODIES IN REGULAR WAVES

TETSUYA MATSUI
Department of Architecture

KENJI KATO
Department of Architecture,
Toyota National Technical College

(Received May 31, 1983)

Abstract

An efficient numerical procedure is described for computing the mean second order wave drift forces on floating axisymmetric bodies in regular waves. It is based on boundary integral and hybrid finite element techniques in potential flow theory. Both far field and near field formulations are employed to derive the expressions for the mean wave drift forces. The axisymmetry of the body geometry is exploited to reduce the computational effort involved. Results based on the present numerical procedure are then compared with the analytical solutions for an articulated circular cylinder and a floating hemisphere. The computational results give close agreement with the analytical ones, thus confirming the validity and accuracy of the present formulation.

1. Introduction

The wave forces acting on a floating structure in irregular waves include the second order, slowly varying components, which are known as the slowly varying wave drift forces. These second order forces, though small in magnitude, can excite long-period resonance motions if the natural period of the mooring system is close to the period of the slowly varying forces.

The reliable prediction of the slowly varying drift forces on structures moored in irregular waves is of critical importance from the point of view of positioning and mooring design. At present, such predictions are usually based on the knowledge of the mean drift forces in regular waves[1,2]. The mean forces can be calculated using results from the first order analysis. Boundary integral and finite element numerical procedures, based on potential flow theory, have been employed in the calculation of the mean drift forces on arbitrary body shapes by Faltinsen and Michelsen[3], Pinkster and Oortmerssen[4], Molin[5] and Standing, Dacunha and Matten[6]. These procedures, however, involve time-consuming computations, associated with the formation of influence coefficient matrices and equation solution for a large number of unknowns. Thus, there is a very practical need for investigating more economical methods of prediction for various special configurations.

One of the most common geometries employed in offshore structures is a vertical body of revolution. Examples include mooring and loading buoys, floating storage tanks, buoyant components of floating platforms, articulated towers for loading or oil production and certain designs of wave energy devices. For these facilities it is possible to apply a more efficient numerical procedure by making use of the axisymmetry of the body geometry. For example, Fenton[7] has formulated a boundary integral approach to calculate wave loads on vertical bodies of revolution, using an axisymmetric Green's function. Employing a similar procedure, Eatock Taylor and Dolla[8] and Isaacson[9] have extended the method to calculate both wave loads and hydrodynamic loads induced by oscillations of the body. A similar formulation using a hybrid finite element approach has been presented by Bai[10] and Chenot[11].

In this paper extension of such a formulation, to permit the computation of mean wave drift forces, is described. Both far field and near field formulations are employed in conjunction with numerical solutions of the first order problem by means of the boundary integral and hybrid finite element techniques. Results based on these numerical procedures are then compared with the analytical solutions for a surface piercing articulated cylinder and a free-floating hemisphere. Some conclusions are drawn regarding the accuracy of the boundary integral and hybrid finite element procedures in the calculation of the wave drift forces.

2. First order solution

2. 1. Basic equations

A rigid vertical body of revolution is considered to be oscillating in an ideal fluid with free surface oxy and constant depth h, as shown in Fig. 1. The axis of symmetry of the body is the coordinate axis oz, measured positive vertically upwards. It is assumed that the body is carrying out a small amplitude periodic motion, in response to excitation by a regular wave propagating in the positive x direction. The motion in the k-th mode is given by

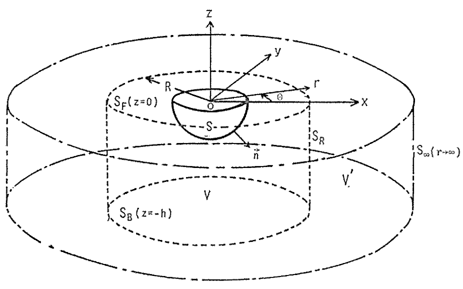

Fig. 1. An axisymmetric body and fluid boundaries.

$$X_k(t)=Re\{x_k e^{-i\omega t}\}, \quad k=1,\ 2,\ 3 \tag{1}$$

where ω is the frequency, t time and x_k is the complex amplitude of motion in the k-th mode. The indices $k=1$, 2 and 3 designate surge, heave and pitch, respectively.

The irrotational fluid motion is characterised by a velocity potential function which at the point M is written

$$\Phi(M,\ t)=Re\{\phi(M)e^{-i\omega t}\} \tag{2}$$

The complex potential $\phi(M)$ may be represented as the sum of three components:

$$\phi=\phi_0+\phi_4-i\omega\sum_{k=1}^{3} x_k\phi_k \tag{3}$$

where ϕ_0 is the incident wave potential, ϕ_4 the scattered wave potential and $\phi_k(k=1, 2, 3)$ the radiation potential, associated with waves induced by unit oscillation of the body in the k-th mode.

In a plane progressive wave of amplitude A and length λ, the incident potential may be expressed in cylindrical coordinates as

$$\phi_0(M)=-\frac{igA}{\omega}\frac{\cosh k(z+h)}{\cosh kh}e^{ikr\cos\theta} \tag{4}$$

where g is the acceleration due to gravity and $k=2\pi/\lambda$ denotes the wave number which is related to the frequency by the dispersion equation

$$\omega^2=gk\tanh kh$$

Equation (4) may also be written as a series of circular waves:

$$\phi_0(M)=\sum_{n=0}^{\infty}\varepsilon_n\phi_0^n(P)\cos n\theta \tag{5}$$

where

$$\phi_0^n(P)=-\frac{igA}{\omega}\frac{\cosh k(z+h)}{\cosh kh}i^n J_n(kr) \tag{6}$$

Here J_n is Bessel function of the first kind of order n and $\varepsilon_0=1$, $\varepsilon_n=2(n>1)$. The scattered and radiated wave potentials may similarly be written

$$\phi_k(M)=\sum_{n=0}^{\infty}\varepsilon_n\phi_k^n(P)\cos n\theta, \quad k=1,\ 2,\ 3,\ 4 \tag{7}$$

These satisfy Laplace equation

$$\nabla^2\phi_k=0 \tag{8a}$$

in the fluid V, the linearised free surface boundary condition

$$\frac{\partial\phi_k}{\partial z}-\frac{\omega^2}{g}\phi_k=0 \tag{8b}$$

on the free surface S_F, and the condition that there is no flow through the sea bottom S_B and the body surface S. The sea bottom condition leads to

$$\frac{\partial \phi_k}{\partial z}=0 \tag{8c}$$

on S_B. On the axisymmetric body, generated by a curve C,

$$\frac{\partial \phi_k^n}{\partial n_c}=h_k^n \text{ for } k=1, 2, 3; \quad \frac{\partial \phi_4^n}{\partial n_c}=-\frac{\partial \phi_0^n}{\partial n_c} \tag{8d}$$

where $\partial/\partial n_C$ denotes the derivative with respect to the outward normal to C. The non-zero terms of h_k^n are given by

$$h_1^1=\frac{1}{2}n_r, \quad h_2^0=n_z, \quad h_3^1=\frac{1}{2}\left[(z-z_G)n_r-rn_z\right] \tag{9}$$

where z_G denotes the z coordinate of the point about which pitch is defined, say the centre of gravity for a freely responding body, and

$$n_r=\partial z/\partial c, \quad n_z=-\partial r/\partial c$$

for a coordinate c measured towards the free surface along C. Furthermore, the scattered and radiation potentials satisfy the radiation condition associated with outgoing waves at infinity:

$$\lim_{kr\to\infty}\sqrt{kr}\left(\frac{\partial \phi_k}{\partial r}-ik\phi_k\right)=0 \tag{8e}$$

For a vertical axisymmetric body having an arbitrary generating curve, numerical approaches such as the boundary integral procedure[7~9] and the hybrid finite element procedure[10,11] may be employed to evaluate the potentials in the form of Eq. (7). These procedures are briefly described in the following sections.

2. 2. Boundary integral formulation

The unknown scattered and radiation potentials of Eq. (7) may be generated by a distribution of sources of varying strength σ_k over the immersed surface of the body:

$$\phi_k(M)=\frac{1}{4\pi}\iint_S \sigma_k(M_0)G(M/M_0)dS, \quad k=1, 2, 3, 4 \tag{10}$$

where M_0 denotes a point on the immersed surface S_B. $G(M/M_0)$ is the Green's function for this problem which may be expressed as a Fourier series in cylindrical coordinates

$$G(M/M_0)=\sum_{n=0}^{\infty}\varepsilon_n g^n(P/P_0)\cos n(\theta-\theta_0) \tag{11}$$

The coefficient g^n have been described by Fenton[7], Eatock Taylor and Dolla[8] and Isaacson[9]. The source strength distribution may similarly be expanded in a cosine series:

$$\sigma_k(M_0)=\sum_{n=0}^{\infty}\varepsilon_n\sigma_k^n(P_0)\cos n\theta_0 \tag{12}$$

Equations (10), (11) and (12) are consistent with Eq. (7) if

$$\phi_k^n(P)=\frac{1}{2}\int_C \sigma_k^n(P_0)g^n(P/P_0)r_0dC \tag{13}$$

since the integration with respect to θ_0 may be performed explicitly.

The unknown source strength distribution must be such that the condition of no flow through the body surface is satisfied. Substitution of Eq. (13) into Eq. (8d) gives

$$-\sigma_k^n(P)+\int_C \sigma_k^n(P_0)\frac{\partial g^n(P/P_0)}{\partial n_c(P)}r_0dC=\begin{cases}2h_k^n & \text{for } k=1,\ 2,\ 3\\ -2\dfrac{\partial\phi_0^n}{\partial n_c}(P) & \text{for } k=4\end{cases} \tag{14}$$

This integral equation may be solved numerically by dividing C into N straight line segments over which the source strength is assumed to be constant. Typical subdivisions for a surface piercing cylinder and a floating hemisphere are shown in Fig. 2. If the boundary condition is applied at one control point on each segment, say the centre of the segment, then Eq. (14) may be replaced by N algebraic equations. Solution of these algebraic equations for each Fourier harmonic leads to the numerical approximations to the scattered and radiation potentials; they are obtained from Eq. (13) by means of a numerical scheme similar to that used in the discretisation of Eq. (14).

2. 3. Hybrid finite element formulation

As shown in Fig. 1, the fluid is divided into two regions by introducing a fictitious vertical cylinder S_R of circular section with radius R which is just large enough to surround the body. The region exterior to S_R will be designated by V' with potential ϕ_k', and the interior fluid region by V with potential ϕ_k. It is easy to show that ϕ_k' may be expressed analytically so as to satisfy Eq. (8a–e) in V'

$$\phi_k'=\sum_{n=0}^{\infty}\varepsilon_n\phi_k'^n\cos n\theta \tag{15}$$

where

$$\phi_k'^n=\alpha_k^{0n}H_n^{(1)}(kr)\cosh k(z+h)+\sum_{m=1}^{\infty}\alpha_k^{mn}K_n(\kappa_m r)\cos\kappa_m(z+h) \tag{16}$$

Here $H_n^{(1)}$ is Hankel function of the first kind of order n, K_n is the modified Bessel function of the second kind of order n, and $\kappa_m(\kappa_1<\kappa_2<\cdots)$ is the positive real roots of the equation

$$\omega^2=-g\kappa_m\tan\kappa_m h$$

It is easy to prove that the following functional

$$J^n(\phi_k^n)=\iint_A\frac{1}{2}\left[\left(\frac{\partial\phi_k^n}{\partial r}\right)^2+\left(\frac{\partial\phi_k^n}{\partial z}\right)^2+n^2\phi_k^n\right]r\,dA-\frac{\omega^2}{2g}\int_{C_F}(\phi_k^n)^2r\,dC_F$$
$$-\int_C\left(\frac{\partial\phi_k^n}{\partial n_c}\right)\phi_k^n r\,dC+\int_{C_R}\left(\frac{1}{2}\phi_k'^n-\phi_k^n\right)\frac{\partial\phi_k'^n}{\partial n_c}R\,dC_R \tag{17}$$

is stational if and only if ϕ_k^n satisfies Eqs. (8a–d) in V and the following matching conditions

$$\phi_k^n = \phi_k'^n, \quad \frac{\partial \phi_k^n}{\partial n_c} = \frac{\partial \phi_k'^n}{\partial n_c} \quad \text{on} \quad S_R \tag{18}$$

as the natural boundary conditions. The functional J^n involves only integrals over a limited area A and its boundaries denoted by C, C_F and C_R, which are defined by the intersections of S, S_F and S_R, respectively, with the $\theta=0$ plane. If ϕ_k^n in A is approximated by finite element representations, the unknown nodal potentials and the unknown coefficients α_k^{0n}, α_k^{mn} in $\phi_k'^n$ may be solved simultaneously by etremizing J^n. Typical finite element idealisations are shown in Fig. 3.

2. 4. Hydrodynamic loads and motion responses

Once the velocity potentials are known, the pressure at any point may be evaluated from the linearised Bernoulli's equation. Hydrodynamic loads are then obtained by integrating the fluid pressure over the surface, immersed in the fluid of density ρ. For the vertical axisymmetric body this leads to the generalised wave forces

$$f_k = -2\pi i \omega \rho \int_C (\phi_0^l + \phi_4^l) h_k^l r \, dC \tag{19}$$

and the added mass and damping matrices, a_{kj} and b_{kj}, respectively, given by

$$a_{kj} + \frac{i}{\omega} b_{kj} = -2\pi \rho \int_C \phi_j^l h_k^l r \, dC \tag{20}$$

where l takes 1 for surge, pitch (k, $j=1$, 3) and 0 for heave (k, $j=2$), These are used with Newton's second law in the formation of equations of motion for the body

$$\sum_{j=1}^{3} [-\omega_2(m_{kj} + a_{kj}) - i\omega b_{kj} + c_{kj} + c'_{kj}] x_j = f_k, \quad k=1,\ 2,\ 3 \tag{21}$$

where m_{kj} is the inertia matrix, c_{kj} is the hydrostatic stiffness matrix and c'_{kj} is the mooring line stiffnes matrix. The non-zero terms of m_{kj} and c_{kj} are given by

$$m_{11} = m_{22} = m, \quad m_{33} = I_y, \quad c_{22} = \rho g A_W, \quad c_{33} = \rho g I_W + mg(z_B - z_G) \tag{22}$$

where m and I_y denote the mass and its moment of inertia (in pitch), respectively, of the body, A_W denotes the water plane area, I_W the moment of inertia of the water plane area A_W about the y axis, and z_B the z coordinate of the centre of buoyancy. The first order body motions are thereby determined by solving the equations of motion.

3. Mean drift forces

3. 1. General remarks

There are currently two approaches that may be used for the computation of drift forces on a floating body in regular waves. The first, generally referred to as the "far field formulation", is based on the calculation of the moment changes within a control surface surrounding the body and extending far away from it. Using the far field velocity potential, one can derive the horizontal drift forces and the moment about a vertical axis, in a relatively simple form. Maruo[12], Newman[13] and Faltinsen and Michelsen[3] have developed the appropriate general expressions. The second approach, known as the "near field formulation" is more direct and may be used to obtain all components of mean drift force and moment. It involves expressing the responses as a perturbation expansion about the mean configuration, integrating the fluid pressure over the varying wetted surface of the body, and retaining terms to second order in the resulting expressions for forces. The formulation has been given by Pinkster and Oortmerssen[4], and may be extended to permit the computation of slowly varying drift forces in bichromatic waves[14]. In the following, the two approaches for the formulation of mean drift forces are used in conjunction with numerical solutions of the first order problem described above.

3. 2. The far field formulation

Following the approach of Newman[13] for deep water, Faltinsen and Michelsen[3] have derived the far field expressions for the horizontal drift forces and moment in finite water depth. The result for the surge drift force is

$$D_x=\left(1+\frac{2kh}{\sinh 2kh}\right)\Big[-\frac{\rho\omega A}{2}Im\{H(0)\}$$

$$-\frac{\rho k^2}{8\pi}\tanh kh\int_0^{2\pi}|H(\theta)|^2\cos\theta d\theta\Big] \tag{23}$$

where $H(\theta)$ is the so-called "Kochin function" defined by

$$\phi(r,\ \theta,\ z)|_{r\to\infty}\sim\left[-\frac{igA}{\omega}e^{ikr\cos\theta}-\sqrt{\frac{k}{2\pi r}}H(\theta)\ e^{ikr-i\pi/4}\right]\frac{\cosh k(z+h)}{\cosh kh} \tag{24}$$

For a vertical axisymmetric body, $H(\theta)$ is expressible as a Fourier series in θ

$$H(\theta)=\sum_{n=0}^{\infty}\varepsilon_n H^n\cos n\theta \tag{25}$$

Equation (24) is consistent with Eqs. (3), (4), (7) (13) and (25) if

$$H^n=-\frac{2\pi iC_0\cosh kh}{k}(-i)^n\int_C\sigma^n(P_0)\cosh k(z_0+h)J_n(kr_0)r_0dC \tag{26}$$

where

$$C_0=\frac{k^2-\nu^2}{k^2h-\nu^2h+\nu} \tag{27}$$

with $\nu=\omega^2/g$, and

$$\sigma^n=\sigma_4^n-i\omega\sum_{k=1}^{3}x_k\sigma_k^n \tag{28}$$

Equation (24) is also consistent with Eqs. (3), (4), (7), (15), (16) and (25) if

$$H^n = -\frac{2\cosh kh}{k}(-i)^n \alpha^{0n} \tag{29}$$

where

$$\alpha^{0n} = \alpha_4^{0n} - i\omega \sum_{k=1}^{3} x_k \alpha_k^{0n} \tag{30}$$

In deriving Eqs. (26) and (29) use has been made of the asymptotic forms of the Green's function and Hankel function for larger r. The Fourier harmonics H^n are thus obtained from numerical solutions of the first order problem. The surge drift force may then be computed from Eq. (23). Integration with respect to θ, after substitution of Eq. (25), yields the far field from of the surge drift force

$$D_x = \left(1 + \frac{2kh}{\sinh 2kh}\right) Re\left\{\frac{i\rho\omega A}{2} H^0 + \sum_{n=1}^{\infty} H^n \left(i\rho\omega A - \frac{\rho k^2 \tanh kh}{2} H^{n-1*}\right)\right\} \tag{31}$$

where * denotes the comlex conjugate.

3. 3. The near field formulation

Pinkster and Oortmerssen[4] have shown how the drift force on a floating body in waves may be obtained by integrating the fluid pressure over the submerged body surface, and retaining terms to second order in a consistent perturbation expansion of the nonlinear equations. This procedure shows that in regular waves the mean drift force may be written as the sum of the four contributions arising from first order effects:

$$\vec{D} = \vec{D}^{\mathrm{I}} + \vec{D}^{\mathrm{II}} + \vec{D}^{\mathrm{III}} + \vec{D}^{\mathrm{IV}} \tag{32}$$

In Eq. (32) $\vec{D}^{\mathrm{I}}$ is caused by the finite relative wave height and is given by

$$\vec{D}^{\mathrm{I}} = -\int_{C_W} \frac{1}{2}\rho g \overline{\zeta_R^2}\, \vec{n}\, dC_W \tag{33}$$

where ζ_R is the total wave elevation relative to the displaced body position, $\vec{n}$ is the unit normal vector directed outwardly from the body, and the overbar denotes the time average. The integration is performed around the intersection C_W of the body and the mean water line.

The contribution $\vec{D}^{\mathrm{II}}$ arises from the pressure drop due to the velocity squared term in Bernoulli equation. It is given by

$$\vec{D}^{\mathrm{II}} = \iint_S \frac{1}{2}\rho \overline{|\vec{\nabla}\Phi|^2}\, \vec{n}\, dS \tag{34}$$

where the integral is performed over the mean wetted surface S, whose normal is $\vec{n}$.

The term $\vec{D}^{\mathrm{III}}$ arises from the product of the gradient of the first order pressure and the first order motion. It may be written

$$\vec{D}^{\text{III}}=\iint_S \rho\overline{(\vec{U}\cdot\vec{\nabla}\Phi_t)}\vec{n}\,dS \tag{35}$$

where $\vec{U}$ denotes the first order motion vector of a point on S. The subscript t on Φ designates the time derivative of Φ.

The final term in Eq. (32), $\vec{D}^{\text{IV}}$, stems from the fact that the direction in which the net first order force acts is altered by the angular motions of the body. This may be related to the inertia forces associated with the first order linear accelerations of a freely responding body of mass m. Thus the term $\vec{D}^{\text{IV}}$ is written as

$$\vec{D}^{\text{IV}}=-\omega^2 m\,\vec{\Omega}\times\vec{X} \tag{36}$$

where $\vec{\Omega}$ is the small rotation of the body and $\vec{X}$ is the vector of translations of its centre of gravity.

For an axisymmetric body, the near field formulation for drift force components may be derived in terms of the Fourier harmonics defined above. The total first order potential is expressed as

$$\Phi(M,\ t)=Re\{\phi(M)e^{-i\omega t}\}=Re\{\sum_{n=0}^{\infty}\varepsilon_n\phi^n(P)\cos n\theta e^{-i\omega t}\} \tag{37}$$

which follows from Eqs. (2), (3), (5) and (7). The gradient of this first order potential is

$$\vec{\nabla}\Phi=Re\left\{\sum_{n=0}^{\infty}\varepsilon_n\left\langle\frac{\partial\phi^n}{\partial r}\cos n\theta,\quad -\frac{n}{r}\phi^n\sin n\theta,\quad \frac{\partial\phi^n}{\partial z}\cos n\theta\right\rangle e^{-i\omega t}\right\} \tag{38}$$

where $\langle\ \ \rangle$ denotes the components of the vector in cylindrical coordinates.

The first order linear motion vector at the point M can be described in terms of the rigid body modes

$$\vec{U}=\langle[X_1+X_3(z-z_G)]\cos\theta,\quad -[X_1+X_3(z-z_G)]\sin\theta,\quad X_2-X_3 r\cos\theta\rangle \tag{39}$$

The relative wave elevation, which accounts for the vertical body motion, is

$$\zeta_R=\zeta-(X_2-X_3 r_W\cos\theta) \tag{40}$$

where r_W is the radius of the body at the mean water level. The wave elevation ζ, measured from the mean water level, may be written in terms of the first order potential

$$\zeta=-\frac{1}{g}\frac{\partial\Phi(M_W,\ t)}{\partial t} \tag{41}$$

where M_W is a point on C_W. The surface elevation relative to the body may therefore be written

$$\zeta_R=Re\{\eta_R e^{-i\omega t}\}=Re\{\sum_{n=0}^{\infty}\varepsilon_n\eta_R^n\cos n\theta e^{-i\omega t}\} \tag{42}$$

where, from Eqs. (1) and (37),

$$\eta_R^0=\frac{i\omega}{g}\phi^0(P_W)-x_2,\quad \eta_R^1=\frac{i\omega}{g}\phi^1(P_W)+\frac{1}{2}x_3r_W,$$

$$\eta_R^n=\frac{i\omega}{g}\phi^n(P_W)\quad (n\geq 2) \tag{43}$$

The point P_W is defined by the intersection of the generator C with the mean waterline.

The time averages in the expression for mean drift force are conveniently written using the relation

$$\overline{Y(t)Z(t)}=\overline{Re\{ye^{-i\omega t}\}Re\{ze^{-i\omega t}\}}=Re\left\{\frac{1}{2}yz^*\right\} \tag{44}$$

The four contributions to the mean drift force on an axisymmetric body may then be obtained by substitution of the foregoing into Eqs. (33)$\sim$(36). The surge drift force, for example, is given by the sum of the following terms:

$$D_x^{\mathrm{I}}=Re\{-\rho g\pi r_W n_r(P_W)\sum_{n=1}^{\infty}\eta_R^n\eta_R^{n-1*}\} \tag{45}$$

$$D_x^{\mathrm{II}}=Re\left\{\int_C \rho\pi r n_r\sum_{n=1}^{\infty}\left[\frac{n(n-1)}{r^2}\phi^n\phi^{n-1*}+\frac{\partial\phi^n}{\partial r}\frac{\partial\phi^{n-1*}}{\partial r}+\frac{\partial\phi^n}{\partial z}\frac{\partial\phi^{n-1*}}{\partial z}\right]dC\right\} \tag{46}$$

$$D_x^{\mathrm{III}}=Re\left\{\int_C \frac{i\rho\omega}{2}\pi r n_r\left[\{x_1+x_3(z-z_G)\}\left(\frac{2}{r}\phi^{2*}+\frac{\partial\phi^{0*}}{\partial r}+\frac{\partial\phi^{2*}}{\partial r}\right)\right.\right.$$

$$\left.\left.+2x_2\frac{\partial\phi^{1*}}{\partial z}-x_3r\left(\frac{\partial\phi^{0*}}{\partial z}+\frac{\partial\phi^{2*}}{\partial z}\right)\right]dC\right\} \tag{47}$$

$$D_x^{\mathrm{IV}}=Re\left\{-\frac{m\omega^2}{2}x_2x_3^*\right\} \tag{48}$$

The corresponding expressions for heave and pitch drift forces may be derived in a similar manner. Although the computations are rather more complex than in the case of the far field formulation, the great advantage of the near field formulation is that it may be employed to obtain all components of mean drift force and moment. Moreover, this formulation may be extended to permit the calculation of slowly varying drift forces in irregular waves.

4. Numerical results

The expressions for the mean drift forces, such as given by Eqs. (31) and (45) $\sim$(48), have been evaluated from numerical first order solutions, based on the boundary integral method (B. I. M.) and the hybrid finite element method (H. E.

M). The computations have been performed for a surface piercing articulated cylinder and a free-floating hemisphere. In both cases the computed results have been compared with the existing analytical solutions.

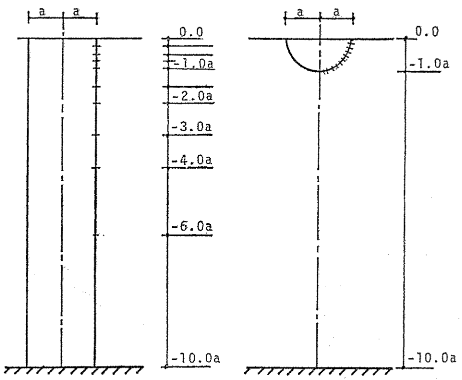

Fig. 2. Typical idealisations for the boundary integral numerical method.

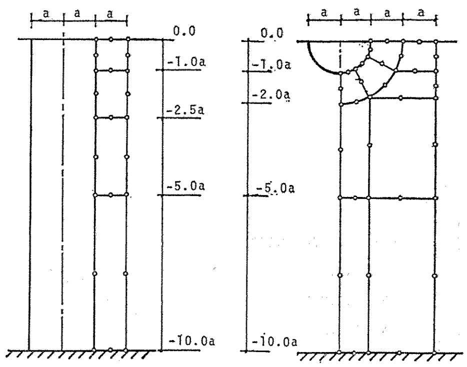

Fig. 3. Typical idealisations for the hybrid element numerical method.

Figs. 2 and 3 illustrate typical idealisations in the boundary integral and hybrid element numerical solutions, presented here. In the B. I. M., the submerged body surface was idealised by 10 or 20 segments (10 segment idealisations are shown in Fig. 2), over which the source strength was assumed to be constant. The integrations over the body surface, associated with the calculation of net fluid forces, were evaluated using a simple trapezoidal formula. In the H. E. M., the interior fluid region was divided into quadratic isoparametric area elements with 8 nodes, while the free surface, body surface and the surface of the fictitious vertical cylinder into quadratic curved line elements with 3 nodes. All integrations were carried out numerically by Gaussian quadrature using 16 points for an area element and 4 points for a line element.

Fig. 4 shows the surge drift force acting on a surface piercing articulated cylinder of circular section, whose radius is one tenth of the water depth. The cylinder is freely responding to a periodic pitching motion about the point of articulation, and the drift force is therefore affected by the first order pitch response. For the purpose of the calculation, the cylinder was assumed to have uniformly distributed mass $0.5\rho\pi a^2$ (a: radius) per unit length in the vertical direction. In this case analytical expressions for the first order solutions may be used to obtain the surge drift force. Thus Drake, Eatock Taylor and Matsui[15] have shown that the far field and near field analytical formulations lead to the identical expression for the surge drift force in deep water

$$D_x=\frac{\rho g A^2}{2k}Re\left\{\sum_{n=1}^{\infty}\left[1-\frac{H_n^{(1)\prime}(ka)H_{n-1}^{(2)\prime}(ka)}{H_n^{(2)\prime}(ka)H_{n-1}^{(1)\prime}(ka)}\right]\right.$$

$$\left.+\frac{2ix_3h}{A}\left(1-\frac{1}{kh}\right)\frac{1}{H_1^{(2)\prime}(ka)}\left[\frac{H_0^{(2)\prime}(ka)}{H_0^{(1)\prime}(ka)}+\frac{H_2^{(2)\prime}(ka)}{H_2^{(1)\prime}(ka)}\right]\right\} \qquad (49)$$

In Fig. 4 results from the far field and near field numerical formulations, based on truncation of the Fourier series at $n=5$, are presented for a range of the values of the dimensionless wave number ka, and compared with the analytical results form Eq. (49).

Fig. 5 shows the surge drift force on a half-immersed free-floating sphere. Both the far field and near field numerical results, retaining Fourier harmonics up to $n=5$, are plotted versus dimensionless wave number. In this case analytical results based on the far field deep water approximation have been obtained by Kudou[16] and are also presented in the figure for comparison.

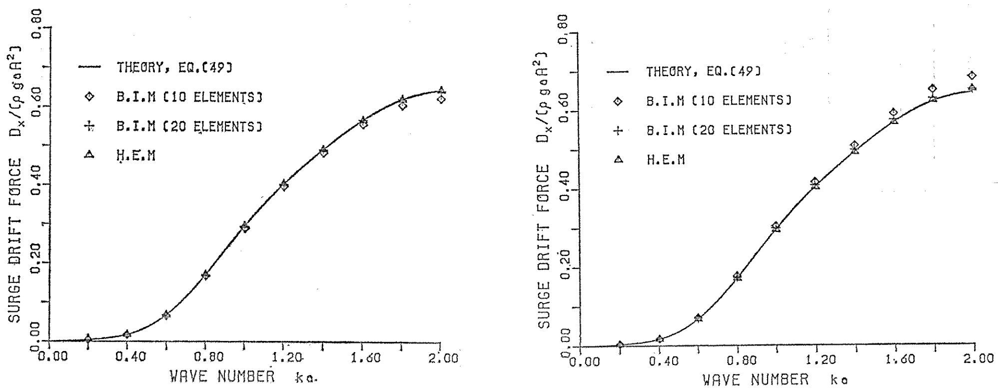

(a) Far field formulation. (b) Near field formulation.

Fig. 4. Surge drift force on a surface piercing articulated cylinder.

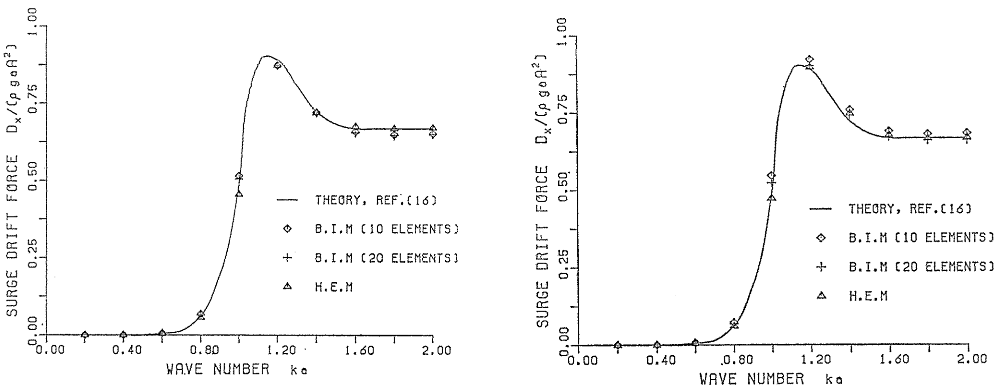

(a) Far field formulation. (b) Near field formulation.

Fig. 5. Surge drift force on a free-floating hemisphere.

The results in Figs. 4 and 5 confirm close agreement between the analytical solutions and the numerical predictions by the B. I. M. and H. E. M. It may be observed that the results obtained from the far field and near field numerical formulations give slightly different values which generally span the analytical solutions from the lower and upper sides.

Table 1 lists the central processor times required in the calculation of one

Table 1. Central processor time. (sec)

	B. I. M.		H. E. M.
	10 elements	20 elements	
Articulated cylinder	1.5	2.6	0.7
Hemi-sphere	1.4	3.4	0.9

frequency. The times quoted were obtained on FACOM M-200 computer at Nagoya University Computation Center. It is clear that the numerical formulations presented in the foregoing provide efficient means for predicting the wave drift forces on an axisymmetric body. By comparing the results from the B. I. M. and H. E. M., one may see that the H. E. M. leads to better accuracy with less CPU time requirements than the B. I. M. This is because the H. E. M. employs quadratic polynomials in interpolating the potential within elements and exploits the symmetry and sparseness of the matrices, while the B. I. M. assumes a constant distribution of the potential over each segment and consumes a great CPU time in the formation of influence coefficient matrix which is generally dense and unsymmetric. From these observations it may be conclued that, in order to assess the second order drift force, which is expressed as products of the first order effects, with sufficient accuracy, it will be useful to adopt numerical schemes based on higher order interpolation functions, as in the H. E. M.

5. Conclusion

In the foregoing the axisymmetry of the body geometry has been exploited to formulate an efficient numerical procedure for calculating the mean wave drift forces on a floating axisymmetric body in regular waves. The validity of the theory and associated computer programs has been confirmed by comparing the results from the present numerical approach with the analytical solutions. The computational effort required will be much less than that for the equivalent three-dimensional approach for arbitrary body shapes. The CPU times listed in Table 1 clearly demonstrate this efficiency.

Only the knowledge of the mean drift forces obtained here is not sufficient for the complete determination of the slowly varying motions in irregular waves. However, the slowly varying excitation forces are generally difficult to evaluate exactly since the second order potential makes an important contribution in this case. The method of evaluating these is now under study[17].

Acknowledgements

A background of this work was carried out while the first author worked for ten months at the Department of Mechanical Engineering of University College London under the support of the Japan Society for the Promotion of Science. The authors would like to thank Dr. R. Eatock Taylor for his suggestion of interesting topics of reseach and valuable discussions. Sincere thanks are due to the financial supports of the Kajima Foundation's Research Grant and a grant from the Takenaka Scholarship Association.

References

1) Hsu, F. H. and Blenkarn, K. A., "Analysis of Peak Mooring Forces Caused by a Slow Vessel Oscillations in Random Seas", *Proc. Offshore Technology Conference, OTC*1159, *Houston* (1970).
2) Pinkster, J. A., "Low Frequency Phenomena Associated with Vessels Moored at Sea", *Society of Petroleum Engineers, SPE*4837, *Amsterdam* (1974).
3) Faltinsen, O. M. and Michelsen, F. C., "Motions of Large Structures in Waves at Zero Froude Number", *Proc. Int. Sympo. on the Dynamics of Marine Vehicles and Structures in Waves, London*, pp. 99–114 (1974).
4) Pinkster, J. A. and Oortmerssen G. van, "Computation of the First and Second Order Wave Forces on Oscillating Bodies in Regular Waves". *Proc. Second Int. Conf. on Numerical Ship Hydrodynamics, Berkeley*, pp. 136–156 (1977).
5) Molin, B., "Computations of Wave Drift Forces", *Proc. Offshore Technology Conference, OTC* 3627, *Houston* (1979).
6) Standing, R. G., Dacunha, N. M. C. and Matten, R. B., "Mean Wave Drift Forces: Theory and Experiment", *National Maritime Institute Report NMI R*124 (1981).
7) Fenton, J. D., "Wave Forces on Vertical Bodies of Revolution", *J. Fluid Mech.*, Vol. 85, Pt. 2, pp. 241–255 (1978).
8) Eatock Taylor, R. and Dolla, J. P., "Hydrodynamic Loads on Vertical Bodies of Revolution", *Trans. Royal Inst. Nav. Arch.*, Vol. 122, pp. 285–297 (1980).
9) Isaacson, M. de St. Q., "Fixed and Floating Axisymmetric Structures in Waves", *Proc. ASCE, J. Waterway, Port, Coastal and Ocean Div.*, Vol. 108, WW2, pp. 180–199 (1982).
10) Bai, K. J., "Zero-Frequency Hydrodynamic Coefficients of Vertical Axisymmetric Bodies at a Free Surface", *J. Hydronautics*, Vol. 11, pp. 53–57 (1977).
11) Chenot, J. L., "Méthode numérique de calcul du mouvement d'un corps flottant soumis à l'influence d'une houle périodique en théorie linéaire", *Rev. Inst. Fr. Pet.*, Vol. 30, pp. 779–802 (1975).
12) Maruo, H., "The Drift of a Body Floating in Waves", *J. Ship. Res.*, Vol. 4, No. 3, pp. 1–10 (1960).
13) Newman, J. N., "The Drifting Force and Moment on Ships in Waves", *J. Ship Res.*, Vol. 11, pp. 51–60 (1967).
14) Pinkster, J. A., "Mean and Low-Frequency Wave Drifting Forces on Floating Structures", *Ocean Engng.*, Vol. 6, pp. 593–615 (1979).
15) Drake, K. R., Eatock Taylor R. and Matsui, T., "The Drift of an Articulated Column in Regular Waves", *Proc. Royal Soc. London* (submitted).
16) Kudou, K., "The Drifting Force Acting on a Three-Dimensional Body in Waves", *J. Soc. Nav. Arch. Japan*, Vol. 141, pp. 71–77 (1977).
17) Matsui, T. and Isobe, T., "The Influence of the Second Order Potential on the Slow Drift Oscillations of Floating Structures", *Proc. 29th Japan Nat. Sympo. Struct. Engng.*, pp. 259–270 (1983).